nature climate change

Article

https://doi.org/10.1038/s41558-024-02201-0

Predictability of abrupt shifts in dryland ecosystem functioning

Received: 7 December 2023

Accepted: 5 November 2024

Published online: 3 January 2025

Check for updates

Paulo N. Bernardino[1,2] ✉, Wanda De Keersmaecker[2,3], Stéphanie Horion[4], Stefan Oehmcke[5], Fabian Gieseke[6], Rasmus Fensholt[4], Ruben Van De Kerchove[3], Stef Lhermitte[1,7], Christin Abel[4], Koenraad Van Meerbeek[1,8], Jan Verbesselt[2,9] & Ben Somers[1,8,9]

Climate change and human-induced land degradation threaten dryland ecosystems, vital to one-third of the global population and pivotal to inter-annual global carbon fluxes. Early warning systems are essential for guiding conservation, climate change mitigation and alleviating food insecurity in drylands. However, contemporary methods fail to provide large-scale early warnings effectively. Here we show that a machine learning-based approach can predict the probability of abrupt shifts in Sudano–Sahelian dryland vegetation functioning (75.1% accuracy; 76.6% precision) particularly where measures of resilience (temporal autocorrelation) are supplemented with proxies for vegetation and rainfall dynamics and other environmental factors. Regional-scale predictions for 2025 highlight a belt in the south of the study region with high probabilities of future shifts, largely linked to long-term rainfall trends. Our approach can provide valuable support for the conservation and sustainable use of dryland ecosystem services, particularly in the context of climate change projected drying trends.

Degradation due to climate and anthropogenic pressure is a major threat to dryland ecosystem integrity and functioning, therefore threatening ecosystems that support about one-third of the global human population[1–4]. Continuous and/or excessive pressure can result in profound alterations in dryland ecosystems functioning[5], causing land degradation and desertification, which in turn, threaten the ability of these ecosystems to function as global carbon sinks[6,7] or provide resources for an ever-growing global population[2]. These alterations can be gradual or accompanied by abrupt shifts[8] and the latter typically occurs due to large perturbations or when conditions (for example, climate, resources) surpass a critical threshold[8–12]. When such a threshold is reached, small perturbations or further changes in conditions can lead to catastrophic shifts in ecosystem functioning[8–10,13] (Supplementary Fig. 1 and Supplementary Table 1). Early warning signals (EWS) for abrupt shifts in ecosystem functioning are, therefore, key information for the early identification of areas at risk, for supporting drylands ecosystem services sustainable use and for the mitigation of climate change effects on drylands[13,14].

In drylands, an important proxy for studying changes in ecosystem functioning is the rain-use efficiency (RUE), that is, the ratio between net primary productivity and rainfall. Because precipitation is the main climatic constraint to vegetation growth in these regions, the RUE can be used to quantify the vegetation–rainfall relationship and therefore serves as a proxy for studying ecosystem functioning and

[1]Division Forest, Nature and Landscape, KU Leuven, Leuven, Belgium. [2]Laboratory of Geo-Information Science and Remote Sensing, Wageningen University, Wageningen, The Netherlands. [3]Remote Sensing Unit, Flemish Institute for Technological Research (VITO), Mol, Belgium. [4]Department of Geosciences and Natural Resource Management, University of Copenhagen, Copenhagen, Denmark. [5]Institute for Visual and Analytic Computing, University of Rostock, Rostock, Germany. [6]Department of Information Systems, University of Münster, Münster, Germany. [7]Department Geoscience and Remote Sensing, Delft University of Technology, Delft, The Netherlands. [8]KU Leuven Plant Institute (LPI), KU Leuven, Leuven, Belgium. [9]These authors jointly supervised this work: Jan Verbesselt, Ben Somers. ✉e-mail: paulo.nbernardino@gmail.com

https://doi.org/10.1038/s41558-024-02201-0

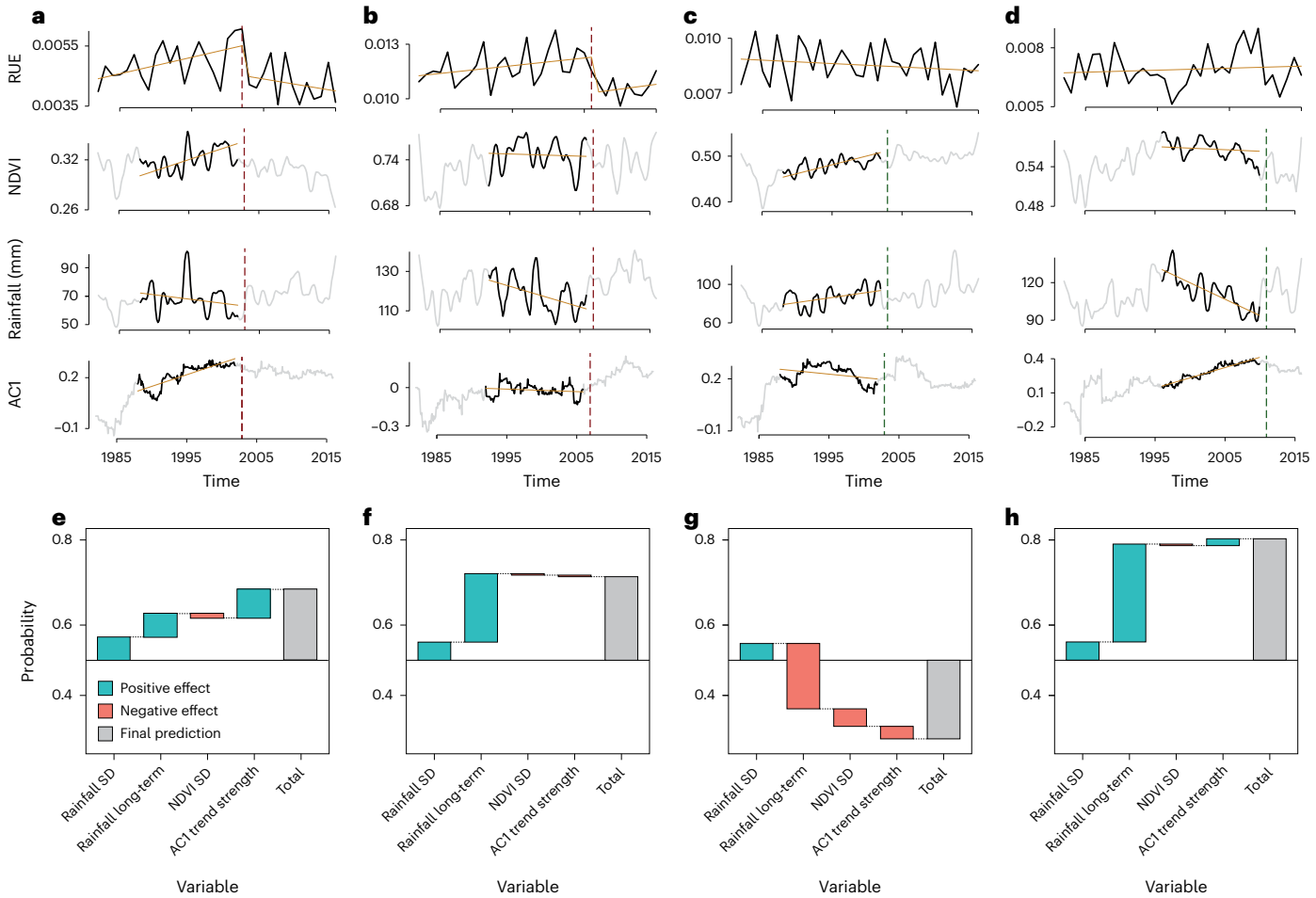

Fig. 1 | Time series examples and how relevant predictors affect abrupt shift occurrence. a–**d**, Time series of RUE and relevant predictor variables: deseasonalized NDVI and rainfall trends and temporal AC1. Examples show pixels where an abrupt shift occurred (**a**,**b**) and did not occur (**c**), correctly predicted by the model; and where it did not occur but the model wrongly predicted an occurrence (**d**). The training period (Methods) is highlighted in black in the time series. The brown lines in the time series are the trend lines. **e**–**h**, The effect of the variables on the model's prediction is presented; the rightmost bar represents the final probability derived by the model: an abrupt shift occurrence is predicted in **e**, **f** and **h**, while in **g** the prediction is that no shift will occur. By relying only on the AC1 trend strength in **b**, no shift would be predicted, whereas combining this information with the other predictor variables resulted in a correct prediction. SD, standard deviation.

land degradation[12,15–17]. Changes in RUE through time can thus indicate alterations in plants' biophysical processes in relation to water availability, ultimately indicating changes in ecosystem functioning[11,12,16]. Thus, by detecting when abrupt changes in RUE occur (that is, a major breakpoint in the RUE time series; Methods), it is possible to determine when the vegetation response to rainfall changed considerably, denoting where and when abrupt shifts in ecosystem functioning have occurred (Fig. 1). Although abrupt shifts were already detected in global drylands[11], an approach to provide effective EWS for these shifts is still missing.

A variety of metric-based approaches for EWS have been developed by, for example, monitoring resilience and critical slowing down[18,19], but their use in large-scale observational studies remains limited due to the challenges imposed by the use of remote sensing data[13,20]. Whereas using increased temporal autocorrelation (that is, slower recovery rates after small perturbations, indicating a loss of resilience) as an EWS works well in controlled experiments or theoretical works[19,21,22], it is challenging to implement autocorrelation as an EWS on satellite time series due to their short length and the presence of noise[20]. Therefore, studies using temporal autocorrelation to predict abrupt shifts or widespread tree mortality based on satellite data are scarce[23], although it is often successfully used as an indicator of resilience changes[24–26]. Moreover, by focusing on one or a few proxies for stability loss among the multitude of available remote sensing and other geospatial data, one might overlook other important signals present in such datasets. For instance, the Normalized Difference Vegetation Index (NDVI) is a proxy for plant productivity, and a strong positive trend in NDVI temporal autocorrelation can be used as an indication that the ecosystem is approaching an abrupt shift. Whereas the absence of such a trend might suggest that the system is far from an abrupt shift, other variables, such as a negative trend in rainfall, might indicate that the system is under pressure and the risk of shifting is imminent.

Machine learning (ML) techniques can potentially resolve some challenges posed by metric-based EWS approaches, due to their ability to find complex patterns in high dimensional data[27–29]. Although ML techniques have been successfully used to predict abrupt shifts in aquatic systems[30,31], their use for predicting abrupt shifts based on satellite data, and in dryland ecosystems more specifically, remains under-explored. Moreover, EWS studies in drylands tend to focus on spatial vegetation patterns and patch size distribution[10,14], whereas studies using temporal metrics are scarce yet fundamental for a comprehensive understanding and successful prediction of abrupt shifts. This is due to the essential information on historical ecosystem response to disturbances from which the model can learn about ecosystems' stability (that is, resistance and resilience) to, for example,

https://doi.org/10.1038/s41558-024-02201-0

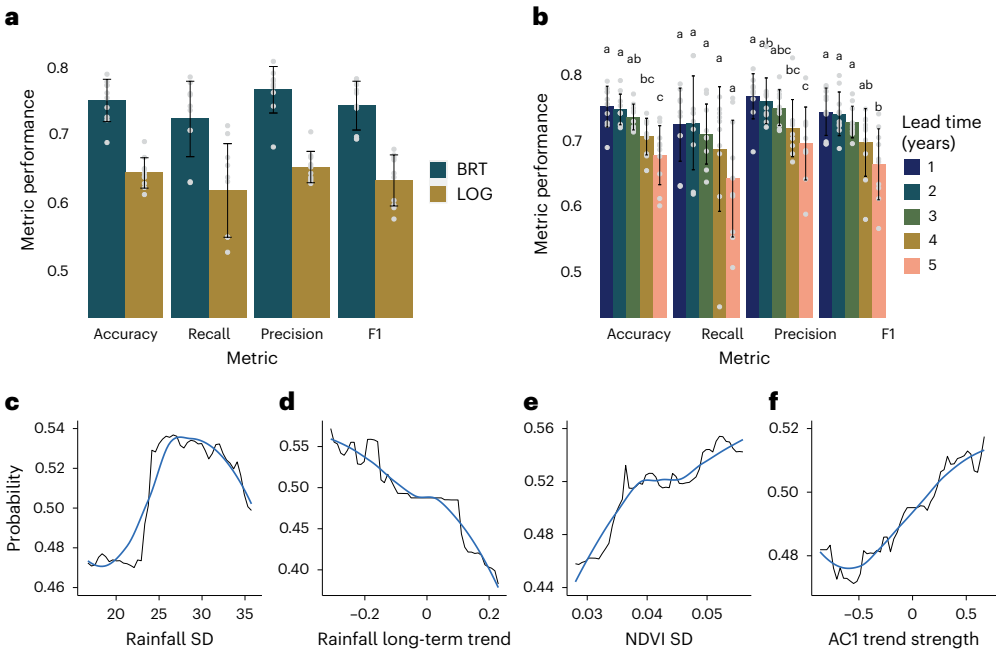

Fig. 2 | BRT model performance and marginal effect plots of predictor variables. a, BRT and logistic regression (LOG) models performances. **b**, BRT model sensitivity to distinct lead times. In both **a** and **b**, evaluation was repeated ten times (Methods); data are presented as mean values ± the standard deviation. Distinct letters represent significant (at $P < 0.05$) differences between groups according to a Kruskal–Wallis followed by a Dunn's post-hoc test. **c**–**f**, Marginal effect plots of rainfall SD (**c**), rainfall long-term trend (**d**), NDVI SD (**e**) and AC1 trend strength (**f**). The LOESS method was used to infer the trend (blue) curves.

climate extremes[32]. Being able to detect areas that are approaching an abrupt shift can support the sustainable use of dryland ecosystems, which could ultimately mitigate food insecurity and support the fight against climate change. Here we present a ML-based approach to detect EWS of abrupt shifts in ecosystem functioning in one of the world's largest dryland regions, the Sudano–Sahelian zone, and show its applicability to identify regions that are more likely to undergo a future abrupt shift. We compared our ML-based approach with a contemporary metrics-based approach based on a logistic regression model trained/evaluated using only temporal autocorrelation (as an EWS) and land-cover information as predictor variables.

Predicting abrupt shifts in the Sudano–Sahel

To predict abrupt shifts in ecosystem functioning, we used a Boosted Regression Trees (BRT) algorithm. Our study area comprises the Sudano–Sahelian zone and areas further to the south, only including water-limited environments (Methods). The model was trained with three conceptually different groups of input variables: first, we used variables related to vegetation and rainfall dynamics (that is, trends and standard deviation), derived from Advanced Very High Resolution Radiometer (AVHRR) Global Inventory Modeling and Mapping Studies (GIMMS) and Climate Hazards Group InfraRed Precipitation with Station (CHIRPS) satellite time series, respectively (Methods), because these might indicate that the ecosystem is unstable or susceptible to changes. Second, we used the strength of the trend in temporal autocorrelation at-lag-1 (AC1) of the vegetation time series as an indicator of resilience loss, because increases in autocorrelation can be used to identify critical slowing down (that is, an indication that the ecosystem is approaching an abrupt shift)[18,19,23]. Third, we used variables related to anthropogenic pressure (for example, population density), drought occurrence, soil characteristics and land-cover type as potential susceptibility indicators (see Methods and Supplementary Table 2 for a complete list of predictors).

On the basis of these input variables and a historical reference dataset of abrupt shift occurrence in the study area[11] (Methods), a BRT model was trained and tested. Model evaluation was performed using a time cross-validation approach[33] because the model will be used to predict the probability of future abrupt shifts. This approach tests models' performance in a future time block not used for training. For instance, training performed for shifts detected in 2001 is tested with shifts detected in 2002. Moreover, to test the sensitivity of our method in predicting abrupt shifts with various lead times (that is, the interval between training period and shift occurrence), we trained and evaluated the BRT model several times with lead times ranging from one to five years. Because temporal cross validation reduces the number of instances used for training the model at each fold, a final model (hereafter BRT_1) was trained using all the available data[33]. Assuming that the additional data is of good quality (for example, correct reference data), the BRT_1 should outperform previously trained models, because more training data are available[33]. However, assessing the accuracy of this model would result in invalid error estimates (that is, the performance would probably be overestimated because no temporal cross validation is executed). Thus, the performance metrics presented here were obtained through the temporal cross validation, being more conservative but also more realistic[33]. Spatial cross validation was also performed to assess if the spatial autocorrelation, present in the predictors, results in overly optimistic accuracies (Appendix 1 in Supplementary Information). Finally, as a benchmark representing the state-of-the-art approach, we used the same temporal cross-validation set-up to train and evaluate a logistic regression model, but only using temporal autocorrelation and land cover as predictors.

Results showed that more than 72% of historical abrupt shifts in ecosystem functioning were predicted correctly (for one-year lead time, overall accuracy: 0.751; recall: 0.723; precision: 0.766; F1 score: 0.743). The relatively high precision indicates that the great majority of the predicted shifts (76.6%) truly occurred. The BRT model performance significantly ($P < 0.05$) decreased as a function of increasing lead times (Fig. 2b), but only when the lead time reached four years. The lack of significant differences between one- and three-year lead time suggests that the model is robust to longer lead times (up to three years) and thus can be used to derive spatially explicit estimates of abrupt shift risk with several years of antecedence. This happens because the most

https://doi.org/10.1038/s41558-024-02201-0

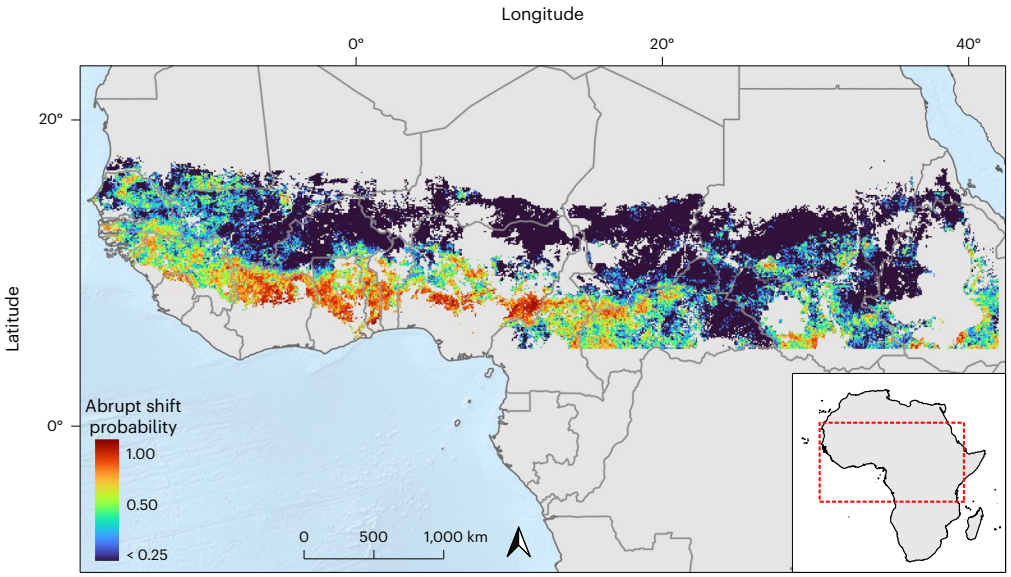

Fig. 3 | Regions with an increased risk of undergoing an abrupt shift in 2025. The map represents abrupt shift probabilities in 2025 estimated by the BRT model trained with a three-year lead time and using NDVI and rainfall data up to 2022 (Methods). Only pixels within water-limited environments were analysed (Methods).

important variables used by the model to predict shifts are either (1) derived using data for several years (for example, the long-term rainfall trend) and thus do not change noticeably when lead time increases or (2) are stable through time (for example, soil characteristics).

Although the BRT model presented a good performance, the false negative rate (observed shifts that were not predicted; 27.7%) was relatively high. Failing to predict observed shifts can be partially explained by the occurrence of abrupt shifts that lack preceding indicators, which can happen, for instance, when no resilience loss precedes the shift. For example, when a large external forcing (for example, vegetation clearing; Supplementary Table 1) causes an abrupt shift, it will occur suddenly and without any prior warnings, and thus, it will not be predictable by the approach applied here. By focusing on accurately differentiating between abrupt shifts caused by the crossing of a critical threshold from the ones caused by large sudden perturbations, future studies might be able to achieve lower false negative rates than the one presented by our model. Other factors that potentially impair the performance of the model are the known limitations of using EWS derived from satellite data (for example, noise in the data and/or too short time series[34]). The model performance decreased when a spatial cross-validation approach was applied (Appendix 1 in Supplementary Information). However, our highest concern here was with the temporal domain, because for future predictions, only past data are available. Meanwhile, the spatial context might in fact add important information for the predictions and should thus be accounted for and not excluded.

To better understand how the BRT_1 model determines abrupt shift probability and to evaluate how differences in key variables make the ecosystem more/less susceptible to a future shift, we analysed variables' importance and produced marginal effect plots for the most important variables. These plots show the marginal effect that a single variable has on the predicted outcome of the model (Methods). Rainfall variability, soil nitrogen, long-term rainfall trend, population density and NDVI variability are the most important input variables for the model's predictions, respectively (Extended Data Fig. 1). These results suggest that by combining information on soil, population density (here used as a proxy for anthropogenic pressure) and vegetation and rainfall variability, we can already identify regions susceptible to abrupt shifts occurrence. Among these variables, only the marginal effect plots for NDVI and rainfall-related variables are shown in Fig. 2 for the sake of simplicity. Plots for soil nitrogen and population density are presented in Extended Data Fig. 2. High levels of rainfall variability (between ± 24 and 33 mm) pose higher susceptibility to a future shift (Fig. 2c). This loss of stability caused by higher levels of rainfall variability may greatly impact Sudano–Sahelian (and dryland) ecosystems, because an increase in rainfall variability is expected in the future due to warmer temperatures[35]. Decreasing long-term rainfall trends increase the susceptibility to future shifts[2,36,37], whereas increasing trends had the contrary effect (Fig. 2d). Differences in the ecosystem's stability due to soil N (Extended Data Fig. 2) are potentially related to soil microbiota-driven resistance[38,39]. An increase in abrupt shift probability is observed as population density increases from 0 to 19 persons per km^2 but stabilizes at higher population density values (Extended Data Fig. 2). This potentially indicates that our approach fails in predicting sudden human-induced shifts in highly populated areas because large stepwise changes cause abrupt shifts without any prior signals[18,34], whereas less intense anthropogenic pressure decreases ecosystems' resilience more slowly, resulting in signals that can be captured by the ML approach. NDVI standard deviation shows an expected behaviour for ecosystems approaching an abrupt shift: disturbances causing flickering and subsequently increasing the variance of the state variable[18,19] (Fig. 2e).

The AC1 trend strength, though less important than other variables (Extended Data Fig. 1), showed expected behaviour found in other studies[18,19,21,23]: higher values indicate an approaching abrupt shift, which translates into higher probability values in the marginal effect plot (Fig. 2f). However, temporal autocorrelation alone is not always a good predictor of abrupt shifts. Thus, the advantage of the multivariate approach proposed here is that when one variable fails to identify an approaching shift, including other relevant variables can overcome this deficiency. For example, in Fig. 1b,f, temporal autocorrelation did not indicate an approaching shift, whereas both rainfall trend and variability did, leading the model to correctly predict the abrupt shift occurrence. The same happened in several other cases. In the testing set, temporal autocorrelation trend strength alone missed 318 instances of actual shifts, but including the remaining predictor variables allowed the model to correctly predict 245 of these instances (77%). Finally, we found that pixels adjacent to others that have undergone abrupt shifts are more susceptible to future shifts. For instance, if one-quarter of the surrounding pixels underwent a shift in a given year, the chance of the target pixel undergoing a shift in the coming year increases by 32.2% (Appendix 2 in Supplementary Information).

ML-based forecasting of abrupt shifts

We applied the BRT model in forecast mode to derive a risk map indicating regions of the Sudano–Sahel that are more susceptible to the occurrence of an abrupt shift in 2025 (Fig. 3). This forecasting was made using a three-year lead time and under the assumption that rainfall and anthropogenic pressure will not change dramatically between 2022 and 2025, the interval between the training period and the year being predicted. This future projection shows that parts of Côte d'Ivoire, Ghana, Benin, Togo and Nigeria are highlighted as more susceptible areas to abrupt shifts in the future. When divided into bioclimatic regions, the Guinean zone presented the largest areas with probabilities higher than 0.5. However, the majority of the study area presents low susceptibility to abrupt shifts in 2025 (values below 0.31), whereas less than 1% of the analysed study area presented extremely high susceptibilities (values above 0.9). In places with high probabilities, the long-term trend in rainfall, which was on average negative for these locations (−0.111 ± 0.137), is identified by the model as the main cause of such high susceptibility. Rainfall variability also appears as a potential cause, with overall high variability levels (32.27 ± 5.54 mm). The marginal effect plots in Fig. 2 indicate that these values are related to high probabilities. In line with this, two large patches with high probabilities are observed in northern Côte d'Ivoire and central Ghana, with average probabilities of 0.84 and 0.83, respectively. These regions have experienced decreasing rainfall trends over the past decades[40–42]. However, it is fundamental to highlight here that even places displaying high-risk levels will not necessarily undergo an abrupt shift in the future. These projections only indicate that current conditions are making the ecosystems in those regions more susceptible, as better discussed below. Local knowledge and a deep understanding of the local factors affecting these ecosystems are necessary, in addition to the regional-scale projections, to generate more accurate predictions at the local scale.

Although abrupt shifts in ecosystem functioning, in general, are interpreted as negative events, they can sometimes be beneficial in ecological and socioeconomic terms. For example, it is widely known that woody encroachment over grasslands can destabilize these ecosystems, leading to losses of functionality (for example, as a source of livestock forage), changes in the water balance and eventually, state shifts[36,43]. A degraded grassland encroached by woody vegetation might present higher primary productivity than a conserved grassland, and thus, higher RUE[44]. In this example, a loss of woody plants in the regeneration process will result in an abrupt drop in RUE, constituting an example of a 'negative' (in the sense that RUE decreases) abrupt shift in ecosystem functioning which is, in fact, positive in ecological and socioeconomic terms. Another example relates to agriculture. Whereas conversion of natural ecosystems to croplands can support livelihoods without grave damage to the environment (that is, when performed at the local scale and sustainably[45]), large-scale and/or negligent conversion can exacerbate drylands' degradation[2,46]. With this in mind, and given the difficulty of determining with coarse-scale satellite data if an abrupt shift is positive/negative at the local scale, we suggest that future work focuses on providing such a qualification based on system-specific characteristics, providing important information for decision-making. Besides, future efforts to establish long-term monitoring field sites, distributed across drylands and focused on the characterization of ecosystems' state and changes in it, are needed. Such data are currently lacking, impeding the use of ground-truth data to validate remote sensing-based large-scale studies on ecosystem shifts such as ours[11,47].

When making predictions with a certain lead time, we assume that ongoing pressures and system conditions will remain constant in the coming years. This is crucial for variables that vary in time and present high importance (Extended Data Fig. 1), such as rainfall long-term trends. For instance, a predicted shift might not occur if unfavourable conditions (during the training period) become favourable afterward. Similarly, whereas population growth trends are relatively stable short-term, they can change in the future. This has two main implications: (1) instead of precisely predicting where abrupt shifts will occur, we focus on estimating future shift susceptibility. Although the shift might not occur in areas with high susceptibility, they are at risk under current conditions. (2) Using accurately modelled and forecasted data for variables such as population density and rainfall can reduce prediction errors. Here because we cannot ensure stable conditions, the predictions represent a risk map, highlighting the near-term risk of major changes in ecosystem functioning based on recent (about 14 years) responses to climate and environmental conditions. Such early warnings are crucial for supporting decisions on ecosystems' sustainable use and climate change mitigation, as they can optimize actions and the use of economic subsidies over areas with a high likelihood of shifting. For that purpose, our results show that ML, combined with relevant predictors, is a powerful tool for providing EWS of abrupt shifts in dryland ecosystem functioning. Although being only a first step towards a fully functional early warning system, our multivariate approach successfully delineated areas more susceptible to future shifts up to three years ahead. Moreover, it correctly predicted, on average, over 75% of the abrupt shifts, including many that would be missed if only temporal autocorrelation trend strength was used as an EWS.

It is well known that drylands are highly endangered by future climate change[2–4], and our results reinforce that increased rainfall variability and decreased rainfall levels can cause widespread abrupt shifts in dryland ecosystem functioning. Also, it is virtually impossible to implement mitigation measures in all dryland regions simultaneously. Thus, by identifying highly endangered areas, policymakers could focus on the most threatened ones. Ultimately, this could contribute to the achievement of UN Sustainable Development Goals (1) No poverty, (2) Zero hunger and (15) Life on land. Our results suggest that areas presenting decreasing trends in rainfall can be more susceptible to abrupt shifts; thus, if combined with future climate projections[48], this indicates that the western Sudano–Sahel will potentially be more susceptible to abrupt shifts in the future due to the projected decrease in rainfall, seen in most of the Coupled Model Intercomparison Project Phase 5 (CMIP5) models[48]. Therefore, action in these areas should be prioritized, aiming at decreasing the risk of ecosystems shifting to a degraded state, which could aggravate poverty and food insecurity in the region[2].

Online content

Any methods, additional references, Nature Portfolio reporting summaries, source data, extended data, supplementary information, acknowledgements, peer review information; details of author contributions and competing interests; and statements of data and code availability are available at https://doi.org/10.1038/s41558-024-02201-0.

References

1. Reynolds, J. F. et al. Global desertification: building a science for dryland development. *Science* **316**, 847–851 (2007).
2. MEA *Ecosystems and Human Well-Being: Desertification Synthesis* (World Resources Institute, 2005).
3. Scholes, R. et al. *Summary for Policymakers of the Thematic Assessment Report on Land Degradation and Restoration of the Intergovernmental Science-Policy Platform on Biodiversity and Ecosystem Services* (IPBES Secretariat, 2018).
4. Easterling, D. R. et al. Climate extremes: observations, modeling, and impacts. *Science* **289**, 2068–2074 (2000).
5. Ponce-Campos, G. E. et al. Ecosystem resilience despite large-scale altered hydroclimatic conditions. *Nature* **494**, 349–352 (2013).
6. Ahlström, A. et al. The dominant role of semi-arid ecosystems in the trend and variability of the land CO_2 sink. *Science* **348**, 895–899 (2015).

7. Fan, L. et al. Satellite-observed pantropical carbon dynamics. *Nat. Plants* **5**, 944–951 (2019).
8. Scheffer, M., Carpenter, S., Foley, J. A., Folke, C. & Walker, B. Catastrophic shifts in ecosystems. *Nature* **413**, 591–596 (2001).
9. Lenton, T. M. et al. Tipping elements in the Earth's climate system. *Proc. Natl Acad. Sci. USA* **105**, 1786–1793 (2008).
10. Berdugo, M., Kéfi, S., Soliveres, S. & Maestre, F. T. Plant spatial patterns identify alternative ecosystem multifunctionality states in global drylands. *Nat. Ecol. Evol.* **1**, 0003 (2017).
11. Bernardino, P. N. et al. Global-scale characterization of turning points in arid and semi-arid ecosystem functioning. *Glob. Ecol. Biogeogr.* **29**, 1230–1245 (2020).
12. Horion, S. et al. Revealing turning points in ecosystem functioning over the Northern Eurasian agricultural frontier. *Glob. Change Biol.* **22**, 2801–2817 (2016).
13. Lenton, T. M. et al. Remotely sensing potential climate change tipping points across scales. *Nat. Commun.* **15**, 343 (2024).
14. Saco, P. M. et al. Vegetation and soil degradation in drylands: non linear feedbacks and early warning signals. *Curr. Opin. Environ. Sci. Health* **5**, 67–72 (2018).
15. Fensholt, R. et al. Assessing land degradation/recovery in the African Sahel from long-term earth observation based primary productivity and precipitation relationships. *Remote Sens.* **5**, 664–686 (2013).
16. Abel, C. et al. The human–environment nexus and vegetation–rainfall sensitivity in tropical drylands. *Nat. Sustain* **4**, 25–32 (2021).
17. Prince, S. D., Wessels, K. J., Tucker, C. J. & Nicholson, S. E. Desertification in the Sahel: a reinterpretation of a reinterpretation. *Glob. Change Biol.* **13**, 1308–1313 (2007).
18. Scheffer, M. et al. Early-warning signals for critical transitions. *Nature* **461**, 53–59 (2009).
19. Dakos, V. et al. Methods for detecting early warnings of critical transitions in time series illustrated using simulated ecological data. *PLoS ONE* **7**, e41010 (2012).
20. Hillebrand, H. et al. Thresholds for ecological responses to global change do not emerge from empirical data. *Nat. Ecol. Evol.* **4**, 1502–1509 (2020).
21. Carpenter, S. R. et al. Early warnings of regime shifts: a whole-ecosystem experiment. *Science* **332**, 1079–1082 (2011).
22. Drake, J. M. & Griffen, B. D. Early warning signals of extinction in deteriorating environments. *Nature* **467**, 456–459 (2010).
23. Liu, Y., Kumar, M., Katul, G. G. & Porporato, A. Reduced resilience as an early warning signal of forest mortality. *Nat. Clim. Change* **9**, 880–885 (2019).
24. Boulton, C. A., Lenton, T. M. & Boers, N. Pronounced loss of Amazon rainforest resilience since the early 2000s. *Nat. Clim. Change* **12**, 271–278 (2022).
25. Verbesselt, J. et al. Remotely sensed resilience of tropical forests. *Nat. Clim. Change* **6**, 1028–1031 (2016).
26. Smith, T. & Boers, N. Global vegetation resilience linked to water availability and variability. *Nat. Commun.* **14**, 498 (2023).
27. Ma, L. et al. Deep learning in remote sensing applications: a meta-analysis and review. *ISPRS J. Photogramm. Remote Sens.* **152**, 166–177 (2019).
28. Maxwell, A. E., Warner, T. A. & Fang, F. Implementation of machine-learning classification in remote sensing: an applied review. *Int. J. Remote Sens.* **39**, 2784–2817 (2018).
29. Ali, I., Greifeneder, F., Stamenkovic, J., Neumann, M. & Notarnicola, C. Review of machine learning approaches for biomass and soil moisture retrievals from remote sensing data. *Remote Sens.* **7**, 16398–16421 (2015).
30. Park, Y., Cho, K. H., Park, J., Cha, S. M. & Kim, J. H. Development of early-warning protocol for predicting chlorophyll-a concentration using machine learning models in freshwater and estuarine reservoirs, Korea. *Sci. Total Environ.* **502**, 31–41 (2015).
31. Robinson, B., Cohen, J. S. & Herman, J. D. Detecting early warning signals of long-term water supply vulnerability using machine learning. *Environ. Modell. Softw.* **131**, 104781 (2020).
32. De Keersmaecker, W. et al. How to measure ecosystem stability? An evaluation of the reliability of stability metrics based on remote sensing time series across the major global ecosystems. *Glob. Change Biol.* **20**, 2149–2161 (2014).
33. Roberts, D. R. et al. Cross-validation strategies for data with temporal, spatial, hierarchical, or phylogenetic structure. *Ecography* **40**, 913–929 (2017).
34. Dakos, V., Carpenter, S. R., van Nes, E. H. & Scheffer, M. Resilience indicators: prospects and limitations for early warnings of regime shifts. *Philos. Trans. R. Soc. B* **370**, 20130263 (2015).
35. Pendergrass, A. G., Knutti, R., Lehner, F., Deser, C. & Sanderson, B. M. Precipitation variability increases in a warmer climate. *Sci. Rep.* **7**, 17966 (2017).
36. Maestre, F. T. et al. Structure and functioning of dryland ecosystems in a changing world. *Annu. Rev. Ecol. Evol. Syst.* **47**, 215–237 (2016).
37. Choat, B. et al. Triggers of tree mortality under drought. *Nature* **558**, 531–539 (2018).
38. Yang, G., Wagg, C., Veresoglou, S. D., Hempel, S. & Rillig, M. C. How soil biota drive ecosystem stability. *Trends Plant Sci.* **23**, 1057–1067 (2018).
39. Delgado-Baquerizo, M. et al. Soil microbial communities drive the resistance of ecosystem multifunctionality to global change in drylands across the globe. *Ecol. Lett.* **20**, 1295–1305 (2017).
40. Atiah, W. A., Tsidu, G. M., Amekudzi, L. K. & Yorke, C. Trends and interannual variability of extreme rainfall indices over Ghana, West Africa. *Theor. Appl. Climatol.* **140**, 1393–1407 (2020).
41. Konate, D. et al. Observed changes in rainfall and characteristics of extreme events in Côte d'Ivoire (West Africa). *Hydrology* **10**, 104 (2023).
42. Kouman, K. D., Kabo-bah, A. T., Kouadio, B. H. & Akpoti, K. Spatio-temporal trends of precipitation and temperature extremes across the north-east region of Côte d'Ivoire over the period 1981–2020. *Climate* **10**, 74 (2022).
43. Schreiner-McGraw, A. P. et al. Woody plant encroachment has a larger impact than climate change on dryland water budgets. *Sci. Rep.* **10**, 8112 (2020).
44. Deng, Y., Li, X., Shi, F. & Hu, X. Woody plant encroachment enhanced global vegetation greening and ecosystem water-use efficiency. *Glob. Ecol. Biogeogr.* **30**, 2337–2353 (2021).
45. Marques, M. J. et al. Multifaceted impacts of sustainable land management in drylands: a review. *Sustainability* **8**, 177 (2016).
46. D'Odorico, P., Bhattachan, A., Davis, K. F., Ravi, S. & Runyan, C. W. Global desertification: drivers and feedbacks. *Adv. Water Resour.* **51**, 326–344 (2013).
47. Cherlet, M. et al. *World Atlas of Desertification: Rethinking Land Degradation and Sustainable Land Management* (Publications Office of the European Union, 2018).
48. Monerie, P. A., Sanchez-Gomez, E. & Boé, J. On the range of future Sahel precipitation projections and the selection of a sub-sample of CMIP5 models for impact studies. *Clim. Dyn.* **48**, 2751–2770 (2017).

Methods

Vegetation and rainfall data

Vegetation dynamics were estimated from time series of Normalized Difference Vegetation Index (NDVI) data obtained from the Global Inventory Modeling and Mapping Studies (GIMMS) NDVI dataset, derived from Advanced Very High Resolution Radiometer (AVHRR) sensors, version 1 (ref. 49). The GIMMS dataset provides bi-monthly NDVI data at about 8 km spatial resolution ranging from July 1981 to December 2015. We used data from 1982 to 2015, to include only full years in our analysis. The maximum value from bi-monthly data was used to generate monthly composites. Monthly rainfall data were retrieved from the Climate Hazards Group InfraRed Precipitation with Station Data (CHIRPS) dataset, with a spatial resolution of approximately 5 km (ref. 50). We selected rainfall data for the period 1982–2015 and aggregated it to the GIMMS 8 km spatial resolution.

From the monthly data, we derived long (entire training period) and short-term trends (first and second halves of the training period) in NDVI and rainfall. The training period is defined in the 'Analysed periods for early warning indicators' section. The NDVI and rainfall time series were detrended and deseasonalized[19] using Seasonal-Trend decomposition using LOESS (STL), leaving us with the NDVI and rainfall remainder (or residuals). Next, NDVI and rainfall standard deviation during the training period were derived from the remainder and used as predictors in the BRT model, because higher variance might indicate the system is unstable[18,19]. The ratio between the NDVI and rainfall standard deviation was also derived and used as a predictor. Finally, temporal autocorrelation at-lag-1 (AC1) was derived and its trend strength was used as an indicator of critical slowing down[18,19]. Monthly autocorrelation values were derived using a Bayesian dynamic linear model and historical (1982–2015) remote sensing NDVI and rainfall data, as proposed by Liu et al.[23]. The model accounts for seasonality in the vegetation and in the climate forcing to derive the AC1[23]. Using the monthly autocorrelation values, the strength of the trend in autocorrelation before the abrupt shift was used as an indicator of an approaching abrupt shift[18,19]. The non-parametric Kendall tau correlation was used to estimate the trend strength (more details in ref. 23).

Land-cover data

Land-cover information was extracted from the majority classes of the MODIS MCD12C1 land-cover product[51] between 2001 and 2015. Considering the existing land-cover classes in our study area, classes defined by the product were aggregated into broader classes: 'evergreen broadleaf forests', 'deciduous broadleaf forests' and 'mixed forests' were grouped as 'forests'; 'closed shrublands' and 'open shrublands' were grouped as 'shrublands'; 'woody savannahs' and 'savannahs' were grouped as 'savannahs'; 'grasslands' remained 'grassland'. Urban areas, croplands and areas without vegetation were masked, as explained below.

Anthropogenic pressure

As proxies of anthropogenic pressure, which together with climate extremes form the major drivers of change in drylands, we used the population density (persons per km^2) in 2015, total livestock density (that is, the sum of cattle, goat and sheep density) in 2010 and the Human Appropriation of Net Primary Production (HANPP) datasets for the year 2000 (the only year available). Population density was obtained from the Gridded Population of the World v.4 (GPWv4) Revision 10 dataset[52], provided at a 5 km spatial resolution and aggregated to the GIMMS NDVI data resolution (~ 8 km). Livestock density was obtained from the Gridded Livestock of the World (GLWv3) dataset[53], provided at the same spatial resolution as the GIMMS NDVI data. The HANPP data were provided by Haberl et al.[54], also at the same spatial resolution as the GIMMS NDVI data. The HANPP is quantified as the aggregated impact of land use on an ecosystem's biomass per year and is an estimate of the human appropriation of nature[54] and thus of the degree of anthropogenic pressure on ecosystems. HANPP values ranged from −358.05 to 848.67 g C m^{-2} yr^{-1}.

Soil data

All soil data were obtained from the International Soil Reference and Information Centre (ISRIC) World Soil Information datasets[55], at a 250 m spatial resolution. Soil variables used here were cation exchange capacity (cmolc kg^{-1}), sand content (g 100 g^{-1}), total nitrogen (g kg^{-1}), total phosphorus (mg kg^{-1}), texture class and depth to bedrock (cm). All data were aggregated to the GIMMS NDVI resolution (~8 km).

Cumulative water deficit

We derived the cumulative water deficit (CWD) using monthly precipitation data (CHIRPS) from 1982 to 2021 following the method of Aragão et al.[56]. The average monthly evapotranspiration was estimated, pixel-wise, using the MOD16A2 v.6 Net Evapotranspiration product[57], provided at a 500 m spatial resolution and aggregated to the GIMMS NDVI resolution (~8 km). The following formula was then used to calculate monthly CWD:

$$\text{If } \mathrm{CWD}_{n-1} - E + P_{\mathrm{n}} < 0;$$
$$\text{then } \mathrm{CWD}_n = \mathrm{CWD}_{n-1} - E + P_n;$$
$$\text{else } \mathrm{CWD}_n = 0$$

where E is the average evapotranspiration, P is precipitation and n is the month. Using the derived CWD, the average and the standard deviation of CWD for each pixel were calculated. Next, standardized anomalies were obtained by subtracting the average value from each month's value and dividing the result by the standard deviation. To determine which months were extremely or severely drier than usual, we assessed the 5th and 15th percentiles of the standardized CWD anomalies, respectively. After this assessment, we defined values below −1.664 as extreme droughts and values between −1.664 and −1.316 as severe droughts. Finally, the total number of months with an extreme and a severe drought were used as predictors in the BRT model.

Study area delimitation

The present study has the Sudano–Sahelian drylands as the prime focus. However, to avoid using rigid boundaries and ensure that the study also comprises ecosystems at the transition between semi-arid and dry sub-humid areas, we extended our analysis to all regions where water is the main limiting factor to plant growth according to Nemani et al.[58]. Thus, the study area extends south of the Sudano–Sahelian zone borders, comprising large parts of the Guinean bioclimatic zone.

Pixels with urban areas and croplands (according to the MODIS MCD12C1 land-cover product[51]) were excluded from our analysis since large-scale human-induced changes can cause abrupt shifts without any signs prior to their occurrence[34] (Supplementary Fig. 1 and Supplementary Table 1). Areas of bare soil and very sparse vegetation (that is, median NDVI < 0.1) were also excluded from the analysis.

Reference dataset of abrupt shifts

Abrupt shifts in ecosystem functioning obtained from Bernardino et al.[11] are used as a reference dataset in this study. This dataset comprises spatial information on the timing, type and significance of abrupt shifts that have occurred between 1982 and 2015, at approximately 8 km spatial resolution in global drylands. The dataset was extended to comprise the study area delimitation defined in the previous section (Extended Data Fig. 3). Below, we summarize key data and methods used to produce the reference dataset. Complete information can be found in refs. 11,12. The ratio between vegetation productivity and rainfall sum during the growing season, that is, the rain-use efficiency (RUE)[59], was used to quantify the vegetation–rainfall relationship[16].

Changes in RUE through time were assumed to indicate changes in dryland ecosystem functioning[11,12]. Abrupt shifts in ecosystem functioning were detected by using a time series segmentation technique, the BFAST01 algorithm[60,61], in the RUE time series. BFAST01 can be used to detect the major breakpoint in a time series, which in the case of the RUE time series indicates the point in time (year) when the vegetation response to rainfall inputs changed markedly, and thus, an abrupt shift in ecosystem functioning[11,12]. Alternatively, abrupt changes in rainfall, not readily accompanied by changes in NDVI dynamics, might also cause abrupt changes in the RUE time series, unrelated to alterations in vegetation biophysical processes. That was, however, not the case in the study area during the period analysed: breaks in the rainfall sum time series (the denominator of RUE) were only detected in 3.5% of the pixels presenting abrupt shifts, and more importantly, only 0.87% of these happened in coinciding years.

Here we focused on predicting only negative abrupt shifts due to two main reasons: (1) we anticipate that including both positive and negative abrupt shifts might add a confounding factor to the model, decreasing its performance; (2) negative shifts were selected because they represent adverse declines in ecosystem functioning, here captured as abrupt decreases in the RUE of an ecosystem[11,12]. It is, however, important to note here that a negative shift cannot be universally interpreted as a shift to a degraded state (discussion in the main text). The final reference dataset, considering the trade-off between data availability and training period length discussed below (Supplementary Fig. 2), contained 2,335 abrupt shift instances.

Analysed periods for early warning indicators

We looked for early warning indicators of abrupt shifts in time series data before the shift occurrence. Because BFAST01 needs data from before and after the abrupt shift to estimate trends and breaks in the trend component, we avoided circularity issues in our analysis by using only data before the abrupt shift occurrence. Fourteen years of data were used to derive the metrics, and with that information, we tested if it was possible to predict the occurrence of an abrupt shift one year ahead (and also two to six years ahead, to test the sensitivity of our approach to distinct lead times). This interval was determined after testing several distinct intervals (that is, 10, 12, 14 and 16-year periods), and because a trade-off between the amount of data points with abrupt shifts and the length of the training interval exists, we selected a suitable period where the data loss was deemed appropriate (Supplementary Fig. 2).

Using the BRT ML model to predict abrupt shifts

In this study, we used the BRT algorithm (XGBoost)[62] to train a model aiming at predicting abrupt shifts in ecosystem functioning. However, more important than actually predicting these shifts, the trained model can produce a risk map highlighting areas susceptible to a future shift. The BRT is similar to a Random Forest, but instead of using the bagging method, which selects instances from the entire dataset completely randomly, the BRT uses the boosting method, weighting instances in a way that poorly modelled data in prior trees have a higher chance of being selected in subsequent ones[62,63]. The BRT model was trained using a reference dataset (containing abrupt shift occurrence as a binary 1/0 categorical variable) and several predictors: (1) indicators of decreased resilience often used to signal an approaching abrupt shift[18,19], (2) proxies for vegetation and precipitation dynamics, (3) environmental variables and (4) proxies for anthropogenic pressure (see Supplementary Table 2 for a complete list of the predictors). Only data before the abrupt shift occurrence, as defined by the reference dataset, were used to derive the predictors (above). We also performed a small test with vegetation and rainfall data to evaluate if the trends observed in the NDVI and rainfall data during the training period hold relevant information on future trends in NDVI and rainfall, respectively, up to five years into the future. A simple approach was used, using the 'auto.arima' function (from the 'forecast' package[64]) to fit an ARIMA model to the data during the 14-year training period, which was then used to forecast NDVI and rainfall trends from one to five years ahead. The root mean squared error (RMSE) for each year was used to evaluate the performance of the predictions. The results of this analysis are presented in Supplementary Fig. 3.

Using abrupt shift occurrence as the response variable and the predictor variables previously specified, the BRT model was then trained. The main goal of training a ML model in this study was to derive probabilities of abrupt shift occurrence in a future year. Therefore, we performed a temporal cross validation, to make sure that the error estimates for the trained BRT model were not overly optimistic[63]. The temporal cross validation was performed by creating time-slice blocks with the same duration and then training a BRT model with one of the blocks. The trained model was then evaluated with a testing set created with data from the upcoming block. For instance, a training set was created using data from 1982 to 1995 to predict abrupt shifts in 1996; the BRT model was trained using these data; a testing set was created using data from 1983 to 1996 to predict shifts in 1997; the BRT model was evaluated using this testing set (that is, the model was trained to predict shifts in 1996 but evaluated by predicting 'future shifts' in 1997). This was iteratively repeated ten times, and at each fold, a random year from the available years with sufficient abrupt shift occurrences (that is, 1996 to 2009) was selected. At each fold, the dataset was under-sampled to correct for imbalances in the number of pixels with and without abrupt shifts (the former was always lower than the latter). The performance metrics (specified below) were then averaged for all the blocks, resulting in a final assessment for the temporal cross-validation model. Time-slice blocks in which the number of training instances was lower than 50 were ignored, because the resulting models would underfit (bad performance on training and test data). This approach allows for a more realistic error estimate for future predictions, and at the same time, avoids an overestimation of the errors in a temporal cross-validation set-up where only the last year (or couple of last years) are left out for the evaluation of the model and the evaluation year(s) are, for some reason, harder to be predicted than all the other years.

Parameter selection for the BRT model was performed using a binary classification problem as objective and aiming at minimizing the classification error. No temporal cross-validation set-up was used for the parameter selection. That is, a random sample containing 75% of the available instances was selected for the training stage, and the remaining 25% of the instances were used for validation. Instances without abrupt shifts were under-sampled to match the number of instances with shifts. The 'xgb.cv' function from the 'xgboost' R package[62] was used, with a 'nfold' of five. The parameters selected were: 0.01 for the learning rate, 7 for the maximum depth of a tree, 1 for the minimum number of instances in each terminal node, 0.8 for the percentage of training data to be sampled for growing trees and 0.8 for the percentage of columns to be subsampled when growing each tree. We set 50 as the number of consecutive rounds without performance improvement needed to stop training, to avoid over-training our model.

The accuracy metrics used to evaluate the model's performance were: the overall accuracy (that is, number of instances correctly classified divided by the total number of instances); the recall (that is, the proportion of abrupt shifts that exist and were correctly predicted, thus penalizing for false negatives but not false positives); the precision (that is, the proportion of predicted abrupt shifts that were correctly predicted, thus penalizing for false positives but not false negatives); and the F1 score (that is, a metric of the balance between recall and precision, calculated as precision multiplied by recall, divided by precision plus recall, multiplied by two). To benchmark against a state-of-the-art approach to predict abrupt shifts, that is, using the temporal AC1 as an EWS for approaching shifts, we used the same set-up explained above to train and evaluate a logistic regression model but using only temporal autocorrelation trend strength and land-cover type as predictor

variables. We added land-cover type as a predictor since we believe that resilience loss might translate into different patterns of AC1 trend depending on the land-cover type being analysed. Therefore, omitting land-cover type from the benchmark model could hamper the prediction ability of the benchmark model due to reasons not related to the use of a multivariate approach (that is, the one used for the BRT model), consequently hampering the comparison between models that we aimed to achieve.

Finally, we trained a final BRT model (the BRT_1) using all the available data, because a higher number of training instances should result, in theory, in a better model[33], considering that the additional data is of good quality (for example, correct reference data). Because the lack of temporal cross validation impairs an accurate performance assessment, the performance obtained from the temporal cross validation (which in theory is more conservative) is presented instead. Moreover, we attempted to minimize the overfitting of the BRT_1 by setting a low learning rate (0.01), sampling a fraction of the available training instances (0.8) for each boosting iteration and sampling a fraction of the predictor variables (0.8) for building each tree[62,63]. The BRT_1 was then used to estimate the predictor variables' importance and derive the marginal effect plots for the relevant variables (main text). These plots show how a variable will overall affect the outcome estimated by the model, that is, if given values of the predictor variable will contribute positively (that is, towards a higher probability of abrupt shift occurrence) or negatively to the final model prediction[63]. Probability values in these plots are not directly translated to abrupt shift occurrence probability; instead, they can be used to detect overall patterns (for example, whether the relationship is linear or nonlinear)[63]. For example, let us consider two pixels in the study area: one presents a long-term rainfall trend value of −0.153 (which represents a probability of 0.523 in the marginal effect plot) and the other a value of −0.328 (which represents a 0.569 probability in the marginal effect plot). The difference between both probabilities is only 0.046 (the second is 9% larger than the first). However, this does not mean that in the final model decision, the difference will be so small. Instead, the actual difference will be 0.335: this variable in the first pixel contributes 0.268 to the final model probability and 0.603 in the second pixel (the second is 125% larger than the first). This happens because models such as the BRT use an ensemble of hundreds of decision trees in which interactions between variables are also considered to make their final prediction[62,63]. Therefore, although the marginal effect plots are important for understanding general patterns, they are made using the marginal effect of a single variable and thus should not be used to infer final predictions. To generate the plots, very high or low values (that is, above and below the 90th and 10th percentiles, respectively) from the predictor variables were omitted to avoid representing in the plots patterns generated with not enough observations. For the specific cases of population density and soil N, because the distribution of the values is right skewed, we removed only very high values, using the 80th percentile.

Because no significant performance loss was observed between the predictions made by models trained with one- to three-year lead time, a BRT_1 model was trained with a three-year lead time (the longest interval without performance loss) for the derivation of future predictions. This model was used in forecast mode to detect areas in the Sudano–Sahel that are more susceptible to the occurrence of an abrupt shift in 2025. For that purpose, we used rainfall data up to 2022 and an extended NDVI dataset (Appendix 3 in Supplementary Information) to derive temporal autocorrelation and vegetation and rainfall dynamics predictors. The derived probabilities were calibrated using Platt Scaling[65].

Data availability

The map with the location and timing of the detected abrupt shifts in ecosystem functioning in the study area is available via Zenodo at https://doi.org/10.5281/zenodo.10636821 (ref. 66). All other datasets used in this study are publicly available from the referenced sources: GIMMS NDVI[49], CHIRPS rainfall data[50], MODIS MCD12C1 land-cover product[51], GPWv4 (ref. 52), GLWv3 (ref. 53), HANPP[54], ISRIC Soil Maps55, MODIS MOD16A2 Net Evapotranspiration product[57].

Code availability

The code used to derive the temporal AC1 from the NDVI and rainfall time series was made available by Liu et al.[23] (https://doi.org/10.1038/s41558-019-0583-9) and adapted to the R language by P.N.B. (https://github.com/paulonbernardino/DLM_example_Liu2019)[67]. Additional custom code used in this study is available via Zenodo at https://doi.org/10.5281/zenodo.10636821 (ref. 66).

References

49. Tucker, C. J. et al. An extended AVHRR 8-km NDVI dataset compatible with MODIS and SPOT vegetation NDVI data. *Int. J. Remote Sens.* **26**, 4485–4498 (2005).
50. Funk, C. et al. The climate hazards infrared precipitation with stations—a new environmental record for monitoring extremes. *Sci. Data* **2**, 150066 (2015).
51. Friedl, M. & Sulla-Menashe, D. *MCD12C1 MODIS/Terra+Aqua Land Cover Type Yearly L3 Global 0.05 Deg CMG V006* (NASA EOSDIS Land Processes DAAC, USGS, 2015); https://doi.org/10.5067/MODIS/MCD12C1.006
52. CIESIN *Gridded Population of the World, Version 4 (GPWv4): Population Density, Revision 10* (NASA SEDAC, 2017).
53. Gilbert, M. et al. Global distribution data for cattle, buffaloes, horses, sheep, goats, pigs, chickens and ducks in 2010. *Sci. Data* **5**, 180227 (2018).
54. Haberl, H. et al. Quantifying and mapping the human appropriation of net primary production in earth's terrestrial ecosystems. *Proc. Natl Acad. Sci. USA* **104**, 12942–12947 (2007).
55. Hengl, T. et al. Mapping soil properties of Africa at 250 m resolution: random forests significantly improve current predictions. *PLoS ONE* **10**, e0125814 (2015).
56. Aragão, L. E. O. C. et al. Spatial patterns and fire response of recent Amazonian droughts. *Geophys. Res. Lett.* **34**, L07701 (2007).
57. Running, S., Mu, Q. & Zhao, M. *MOD16A2 MODIS/Terra Net Evapotranspiration 8-Day L4 Global 500 m SIN Grid V006* (NASA EOSDIS Land Processes DAAC, 2017); https://doi.org/10.5067/MODIS/MOD16A2.061
58. Nemani, R. R. et al. Climate-driven increases in global terrestrial net primary production from 1982 to 1999. *Science* **300**, 1560–1564 (2003).
59. Le Houérou, H. N. Rain use efficiency: a unifying concept in arid-land ecology. *J. Arid. Environ.* **7**, 213–247 (1984).
60. Verbesselt, J., Hyndman, R., Newnham, G. & Culvenor, D. Detecting trend and seasonal changes in satellite image time series. *Remote Sens. Environ.* **114**, 106–115 (2010).
61. De Jong, R., Verbesselt, J., Zeileis, A. & Schaepman, M. E. Shifts in global vegetation activity trends. *Remote Sens.* **5**, 1117–1133 (2013).
62. Chen, T. & Guestrin, C. Xgboost: a scalable tree boosting system. In *Proceedings of the 22nd ACM SIGKDD International Conference on Knowledge Discovery and Data Mining* 785–794 (Association for Computing Machinery, 2016).
63. Hastie, T., Tibshirani, R. & Friedman, J. *The Elements of Statistical Learning—Data Mining, Inference, and Prediction* (Springer, 2009).
64. Hyndman, R. J. & Khandakar, Y. Automatic time series forecasting: the forecast package for R. *J. Stat. Softw.* **27**, 1–22 (2008).
65. Platt, J. C. Probabilistic outputs for support vector machines and comparisons to regularized likelihood methods. *Adv. Large Margin Classifiers* **10**, 61–74 (1999).

66. Bernardino, P. N. et al. Predictability of abrupt shifts in dryland ecosystem functioning. *Zenodo* https://doi.org/10.5281/zenodo.10636821 (2024).
67. Bernardino, P. N. DLM example from Liu, et al. 2019 translated to R. *GitHub* https://paulonbernardino.github.io/DLM_example_Liu2019 (2020).

Acknowledgements

We would like to acknowledge the following funding agencies for the provided financial support: Belgian Science Policy Office (grant SR/00/339; P.N.B., W.D.K., S.H., R.F., R.V.D.K., S.L., J.V., B.S.); Villum Fonden (grant 37465; S.H.); Independent Research Fund Denmark (grant 2032-00026B; R.F.); European Space Agency (ESA) as part of the Climate Change Initiative (CCI) fellowship (ESA ESRIN/contract number 4000133555; C.A.); University of Copenhagen (Data+ grant PerformLCA; S.H., S.O.); German Federal Ministry of Education and Research (grant 01IS23025A; F.G.). We would like to thank R. S. Oliveira for the insights provided.

Author contributions

P.N.B., W.D.K., S.H., R.F., R.V.D.K., S.L., J.V. and B.S. conceived the study. P.N.B., W.D.K., S.H., R.F., R.V.D.K., S.L., J.V. and B.S. contributed to initial ideas. P.N.B, W.D.K., S.H., S.O. and F.G. performed data processing. P.N.B., W.D.K., S.H., S.O., F.G., R.V.D.K., S.L. and K.V.M. designed and conducted analyses. P.N.B., with the assistance of W.D.K., S.H., K.V.M. and C.A., wrote the first draft. All the authors contributed to additional versions.

Competing interests

The authors declare no competing interests.

Additional information

Extended data is available for this paper at https://doi.org/10.1038/s41558-024-02201-0.

Supplementary information The online version contains supplementary material available at https://doi.org/10.1038/s41558-024-02201-0.

Correspondence and requests for materials should be addressed to Paulo N. Bernardino.

Peer review information *Nature Climate Change* thanks Thomas Bury, Niall Hanan and Max Rietkerk for their contribution to the peer review of this work.

https://doi.org/10.1038/s41558-024-02201-0

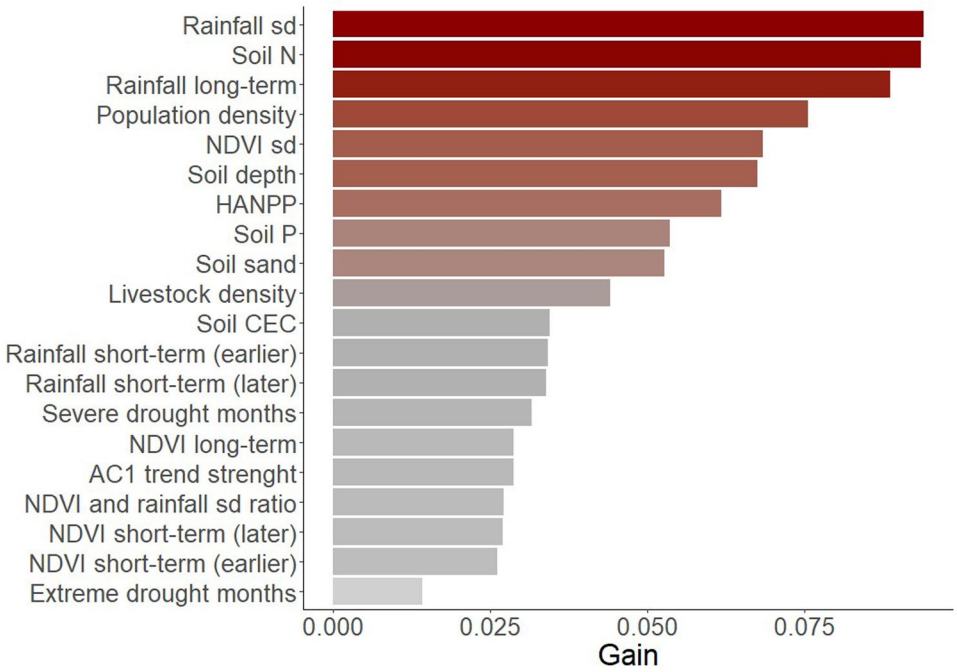

Extended Data Fig. 1 | Importance of the variables used by the BRT model. To assess each variable's importance, we used here the gain value. 'Long-term' refers to the entire 14-years training period, while 'short-term (earlier)' refers to the first seven years and 'short-term (later)' to the last seven years. N: nitrogen; sd: standard deviation; HANPP: human appropriation of net-primary productivity; P: phosphorus; AC1: autocorrelation at-lag-1; CEC: cation exchange capacity.

https://doi.org/10.1038/s41558-024-02201-0

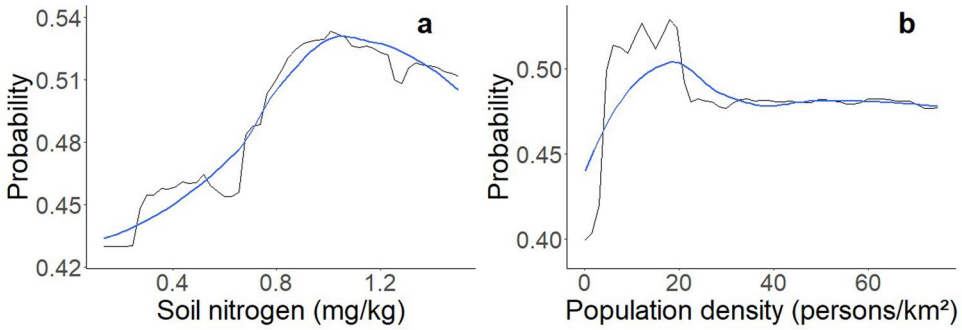

Extended Data Fig. 2 | Marginal effect plots for soil nitrogen and population density. These variables represent the second and fourth most important variables used by the BRT model. Abrupt shift probability increases with soil nitrogen (**a**), while for population density (**b**), an increase is observed up to 19 persons/km^2, but then probabilities stabilize around 0.48 at 32 persons/km^2.

https://doi.org/10.1038/s41558-024-02201-0

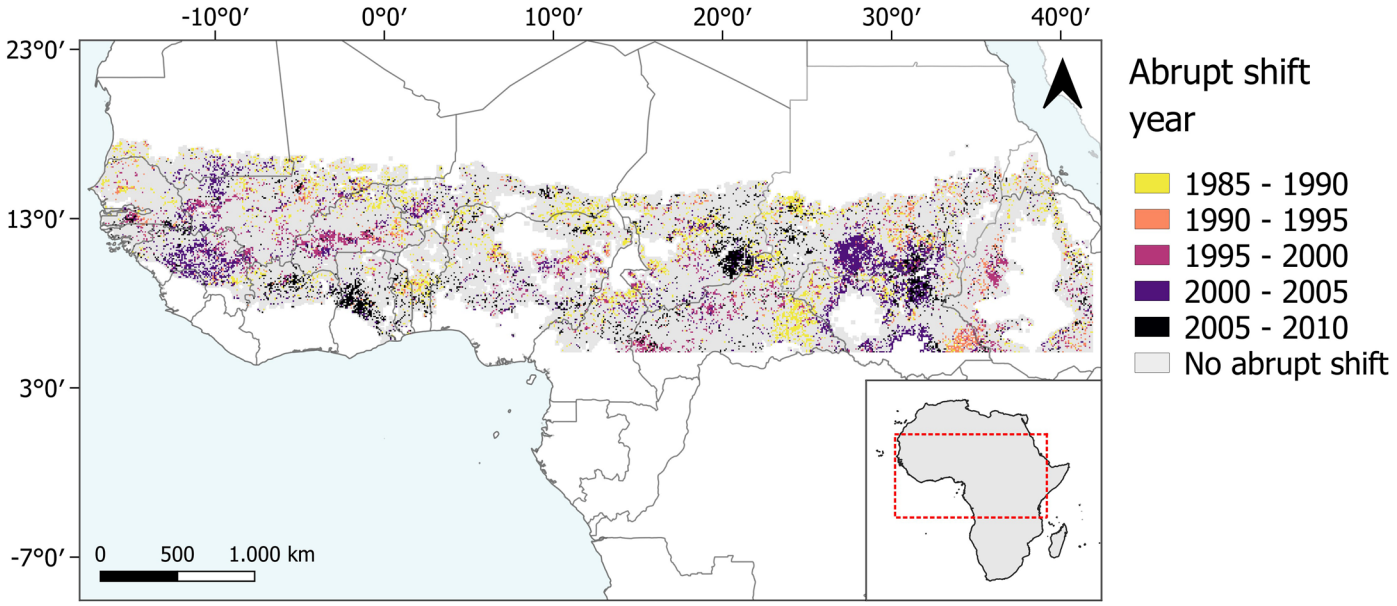

Extended Data Fig. 3 | Updated map with the detected abrupt shifts, and their respective years, for the study area. When compared to the results of Bernardino et al.[11], the updated map presents abrupt shifts detected in regions that are located south of the Sudano-Sahel, but that are still mainly limited by water availability (see Methods).